

A SOLAR REFRIGERATION SYSTEM'S PERFORMANCE IMPROVEMENT FOR A VARIABLE THROAT EJECTOR

Muddu Allaparthi¹, K. Sudha Madhuri², Sandhya Rani Borukati³, Ajith Rai⁴, Haridasu Deepti⁵, T. Lokeshwar Rao⁶

¹Assistant Professor, Department of Mechanical Engineering, R.V.R & J. C. College of Engineering, Guntur, India

²Associate Professor, RGM CET, Nandyal

^{3,5,6}Assistant Professor, Dept. of Mechanical Engg., Malla Reddy College of Engg. & Tech., Hyderabad, India

⁴Assistant Professor, Dept. of Aeronautical Engg., Malla Reddy College of Engg. & Tech., Hyderabad, India

Abstract:

It can be challenging to maintain a constant generator temperature in a solar vapour ejector refrigeration system because fluctuations in solar irradiation intensity can affect the solar heat supply. This work suggests a variable throat ejector (VTEJ) to enhance ejector performance and evaluates its performance using CFD simulations. One can infer the following conclusions. Although it may be overdesigned and costly, an ejector with a bigger throat area and solar collector offers a broader working range of generator temperatures. On the other hand, reducing the throat area reduces the temperature range across which the generator may operate. As a result, using solar energy as a heat source may not be possible for the ejector with a set throat area. The ideal throat area ratio and operating temperatures are derived for a VTEJ in this work using a curve-fitting method. The ejector can continuously achieve optimal and steady performances under a variable solar heat source by using this equation to modify the throat area ratio.

Keywords: Refrigeration system, Throat ejector, solar vapour ejector, Solar collectors, and Throat ratio.

1. Introduction

The refrigerant enters the solar collector of a typical vapour ejector refrigeration system, flows through it, and finally escapes as vapour. The collector serves as the refrigeration system's vapour generator in addition to gathering heat from the sun [1]. However, differences in solar irradiation intensity may induce variations in the quantity of solar heat supplied to the collector, [2] making it challenging to maintain a constant generator temperature. During system operation, the temperatures of the condenser and evaporator may also change. The ejector geometry and operational circumstances affect how well an ejector-refrigeration system performs. By adjusting the operating temperatures, such as the generator temperature, evaporator temperature, and condenser temperature, one may alter the ejector performance, which includes the entrainment ratio (E_m), coefficient of performance (COP), and critical condenser temperature (T_{cr}) [3]. A refrigeration system's ejector should have a certain shape for a particular operating situation in order to work at its best [4]. Because of this, a traditional fixed

geometry ejector that employs solar energy as a heat input is unable to work at its best. It seems sense to make the ejector design flexible to account for variations in operating circumstances in order to improve the refrigeration system.

The use of varying ejectors in refrigeration systems can produce optimal performance under a variety of operating situations, according to a survey of the literature on the subject.[5] investigated this idea using a one-dimensional (1-D) ejector theory. The conventional 1-D gas dynamic theory has been used to construct and study ejectors[6]. By assuming the relevant subcomponent efficiency, losses in the main nozzle, secondary nozzle, mixing chamber, and diffuser are taken into account using this technique. These empirical loss coefficients, which are dependent on the ejector geometries, may found by correlating experimental results [7, 8]. In order to do this, the current article concentrates on creating a suitable methodology to optimise the ejector geometry in a two-dimensional (2-D) geometry.

Various types of ejectors have lately been researched using CFD in order to replicate the ejector flow in a more realistic manner than with 1-D theory. CFD has been demonstrated by [9] to be an effective and precise method that offers adequate detail information for ejector design. This work suggests a variable throat ejector (VTEJ) to enhance ejector performance and evaluates its performance using CFD modelling. A variable throat ejector can also increase ejector efficiency in vehicle hydrogen fuel cell systems, as demonstrated experimentally and computationally by [10]. Depending on the operating environment, their design alters the ejector throat area ratio. They did not, however, address the ideal ejector geometry. To alter the throat area, they employed a needle-like cylinder cone that protruded into the major throat part from the downstream. The downstream needle and supersonic flow may, however, combine to produce a complicated shock wave. Additionally, the cross-sectional size of the needle restricts the flow velocity of the refrigerant travelling through the ejector, which might negatively impact the ejector's function.

The VTEJ being studied in this paper has a spindle with a changeable cross section along the axis[11]. The spindle is introduced into the main nozzle from the upstream side in order to reduce the impact of the intruding spindle [12, 13]. The major throat region is altered as a result of changing the spindle's location. An unstable solar heat source can be accommodated by this controlled spindle adjustment. The primary goal of this study is to statistically examine the VTEJ's capacity to perform at its best throughout a wide range of operational temperatures.

2. Method

The VTEJ generally experiences turbulent, compressible fluid flow. This work uses the k-turbulence model to explain the turbulent behaviour in the VTEJ and assess the fluid field characteristics. We also concentrate on 2-D steady flow analysis. The following operating parameters are used in this study: (1) a generation temperature, T_g , ranging between 90 and 110 0C; (2) a condenser temperature, T_c , surpassing 35 0C; and (3) an evaporator temperature, T_e , ranging between 12 and 20 0C. R245fa is the working fluid[14]. VTEJs disregard heat transmission via their walls.

The suggested ejector's dimensions are shown in Table 1 and Fig. 1. The ejector in the mixing chamber has a converging angle to enhance the E_m . A higher E_m was obtained by simulating

the nozzle exit position (NXP). Different throat area ratios, range from 5.7 to 12.0, were simulated, where $Ar = A_3/A_t$ (the ratio of the secondary throat area, A_3 , to the main throat area, A_t). The ejector was created using FLUENT 6.3, a commercial CFD software. A 2-D axisymmetric solver was used to model the ejector. The mesh was composed of triangular pieces, however the boundary layer next to the wall had quadrilateral elements. A denser grid is necessary due to the complicated flow pattern in the entrainment region, which is caused by the interaction of the shock wave and boundary layer. The adaptive mesh was used in the area of the shock wave since the shock wave position fluctuates with the change in operating circumstances. The close-to-wall region was handled like a typical wall function. It was presumed that the operating fluid was an ideal gas. Other characteristics stayed the same throughout the simulation. The boundary conditions were all configured as pressure boundaries.

NXP	d1	L1	ds	Ls	d2	L2	d3	L3	dd	Ld
30	13.8	41.2	68	36.66	22.48	19	99.87	34	114.5	114

A_r	A_3	VTEJ_ A_t	Move forward
7.2	283.385	39.359	12.838
9.4	283.385	30.359	20.436
12	283.385	23.615	24.431

2.1 Experimental Setup

The trials were carried out on an ejector experimental setup with a cooling load of 10.5 kW (3RT). The experimental setting is described in detail in [15]. The experimental ejector, a generator, an evaporator, a condenser, a receiver-subcooler, a float regulating valve, a gear-type feed pump, a cooling tower, and a control panel with various measuring instruments were the nine main parts of the ejector test rig equipment. Glass level gauges were used in the cylinder-shaped construction of the generator and evaporator to monitor the liquid level. Two 13 kW electric heaters that have been individually regulated heated the operating fluid of the generator. Two 6 kW electric heaters were used to replicate the evaporator cooling load by transferring heat directly to the evaporator. A typical shell-and-tube exchangers with a glass level indicator, the condenser had a 52 kW reject heat capacity and was cooled by water from the cooling tower. The receiver-subcooler was a specifically made vertical vessel of the shell-and-coil type that used cooling tower water to keep it cold. It had a level gauge and a level transmitter for monitoring and controlling the liquid level. The generator feed pump was a hydraulic gear-type pump powered by a three-phase, variable speed electric motor. Gear-type flow metres were used to monitor the primary and secondary flow rates. The building of the ejector test rig also included a control panel with various instruments and other common refrigeration machine components. For the ejector test rig, a PC-based monitoring and control system was created. A data collecting system collected the data every 10 s. The findings were

computed using the pressures, temperatures, primary and secondary flow rates, electric power consumptions, and other necessary data that were recorded. This made it possible to identify the key performances under system operating conditions that were steady state.

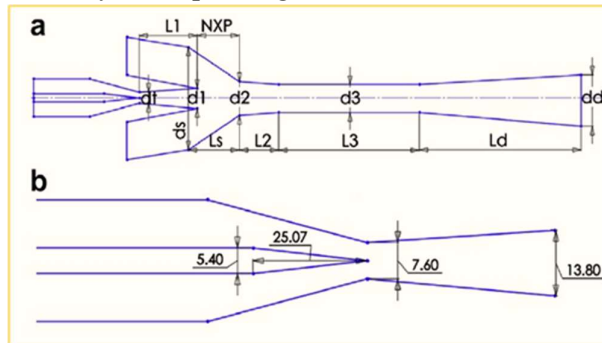


Fig 1. Ejector Geometry

Cells of mesh	$T_{cr}(^{\circ}C)$	$E_m(\%)$	$Q_e(kW)$	COP
39592	37.6	50.3	3.91	0.372
51481	38	52.8	4.07	0.391
75526	38	52.6	4.06	0.389

2.2 Independent grid test

The grid independence test results for one of the suggested ejectors with an area ratio of 8.6, $T_g = 100\text{ C}$, and $T_e = 15\text{ C}$ are shown in Table 2. As the number of mesh cells rises, there is only a very little change in the E_m , cooling load (Q_e), and COP. As a result, all of the simulations were run with around 50,000 cells in order to save processing time.

3. Results and Discussions

This study initially talks about the E_m and COP performances for fixed-throat-area ejectors in section 3.1, where the throat area ratio is taken into account. Second, the effectiveness of Sections 3.2-3.5 analyse E_m and COP for VTEJs. Then, corresponding to various throat area ratios, the heat supply and cooling load are studied. The results that are provided, as mentioned, were all acquired quantitatively.

$T_g(^{\circ})$	A_r	$E_m(\%)$	$Q_g(kW)$	$Q_e(kW)$	COP
90	7.2	57	9.82	4.27	0.43
100	7.2	40.1	12.53	3.73	0.3
110	7.2	33.6	15.72	3.43	0.24

3.1 Performance of ejectors with a fixed throat area

The impact of changing generator temperatures on ejector performance is covered in this section. Temperatures for the evaporator and condenser were maintained at $15\text{ }^{\circ}C$ and $35\text{ }^{\circ}C$, respectively. Analysis was done on three fixed area ratios of 7.2, 9.4, and 12. It is feasible to highlight the benefits and drawbacks brought on by various area ratios after looking at the E_m ,

COP, cooling load, and necessary generating heat. It is also conceivable to explain the need for a variable throat ejector in order to prevent fixed ejectors' inefficiency when the generator temperature changes due to varied solar irradiation. The ejector's performance with the throat area ratio set at 7.2 while the generator temperature changes. When the generator temperature is between 90 and 110 C, this ejector acts as choked with a slight variation in cooling load.

Table 4 - Ejector performance with throat area ratio fixed at 9.4, $T_c=35\text{ }^{\circ}\text{C}$ & $T_e=15\text{ }^{\circ}\text{C}$

$T_g(^{\circ})$	A_r	E_m (%)	$Q_g(\text{kW})$	$Q_e(\text{kW})$	COP
90	9.4	Reversed flow			
100	9.4	60.8	9.65	4.36	0.45
110	9.4	44.01	12.14	3.87	0.32

Table 5- Ejector performance with throat area ratio fixed at 12.0, $T_c=35\text{ }^{\circ}\text{C}$ & $T_e=15\text{ }^{\circ}\text{C}$

$T_g(^{\circ})$	A_r	E_m (%)	$Q_g(\text{kW})$	$Q_e(\text{kW})$	COP
90	12.0	Reversed flow			
100	12.0	Reversed flow			
110	12.0	68.3	9.4	4.67	0.50

This is due to the secondary flow, which is entrained into the mixing chamber, not appreciably changing with differing generator temperatures at the choked condition. Because of the increased pressure at the primary nozzle's input, the main nozzle flow rate rises along with the generator temperature. As a result, it causes a drop in E_m and COP and an increase in Q_g and the heat supply. The table also demonstrates that when the generator temperature reaches 110 $^{\circ}\text{C}$, the solar collector's heat output is at its highest. The amount of heat needed is 1.60 times greater at this temperature than it is at 90 $^{\circ}\text{C}$. The size of the solar collector must be chosen based on the highest heat required, which is the one running at the generator temperature of 110 $^{\circ}\text{C}$ instead of 90 $^{\circ}\text{C}$, to enable the ejector system with the throat area ratio fixed at 7.2 to work at generator temperatures ranging from 90 to 110 $^{\circ}\text{C}$. For such a system, the solar collector provides just enough energy to evaporate the refrigerant if the ejector system runs at 110 $^{\circ}\text{C}$. The solar energy is surplus if the ejector system runs at a temperature below 110 $^{\circ}\text{C}$. The amount of heat needed by the VTEJ when the generator temperature is between 90 and 110 $^{\circ}\text{C}$, as mentioned in Section 3.2, is the same as when the fixed ejector is running at 90 $^{\circ}\text{C}$ rather than 110 $^{\circ}\text{C}$. The amount of heat required at 90 $^{\circ}\text{C}$ is 60% less than at 110 $^{\circ}\text{C}$. Therefore, when the generator temperature is below 110 $^{\circ}\text{C}$ for this ejector system with such a fixed throat area ratio of 7.2, the solar collector is oversized. Table 3 displays the ejector's performance as the generating temperature changes with the throat area ratio set at 9.4. When the generator temperature reaches 90 C, this system cannot operate because the critical condenser temperature is below the working temperature of 35 C. The system enters a failure condition and produces no cooling load as a result of the fluid in the mixing chamber flowing back to the

evaporator. With a slight adjustment in cooling load, the system can still function when choked when the generator temperatures is between 100 and 110 0C. The current ejector, which has a smaller throat size (or greater area ratio) than the previous one in Table 3, that has a greater throat area (or lower area ratio), has a higher E_m and COP. Additionally, it demonstrates that a smaller solar collector is needed since the generator uses less heat. In conclusion, an ejector system with the a smaller throat area can perform better and is more economical, but the drawback is that the generator's working temperature can only be within 100 and 110 C. Table 5 displays the ejector's performance as the generator temperature varies with the throat area ratio set at 12.0. When the generator temperature is between 90 and 100 C, this system cannot run in the choked situation. Only when the generator temperature reaches 110 C can it run in the clogged state. The current ejector achieves the greatest E_m and COP when compared to the two prior ejectors with greater throat regions (Tables 3 and 4). The smallest solar collector and least amount of heat are needed by this generator. In conclusion, the ejector with the shortest throat area performs best and is the most economical, but on the negative, it has the generator's narrowest working temperature.

In conclusion, a bigger throat area combined with a larger solar collector provides for a broader range of generator operating temperatures, but may be overdesigned and costly for the ejector with a fixed throat area. The working range of the generator temperature does, however, drop as the throat area is reduced. As a result, using solar energy as a heat source may not be feasible for the fixed throat area ejector.

3.2 Variable throat ejector

By introducing a spindle with a changeable cross section into the main nozzle, the suggested ejector may change the throat area. The spindle's location may be changed to create various throat regions. Based on the outcomes from the fixed throat ejectors in Section 3.1, the throat area ratio is calculated for each generator temperature. Table 6 displays the throat area ratio that has to be changed in relation to generator temperature and the VTEJ's related performance. The temperature of the crucial condenser is still higher than 35 C. As a result, the system can function while the generator is clogged at temperatures between 90 and 110 C. As the generator temperature changes, the VTEJ's heat supply and cooling load essentially remain unchanged, and at a generator temperature of 90 C, the VTEJ's heat supply is practically identical to that of a fixed throat ejector with an area ratio of 7.2. Therefore, it is clear that the variable throat ejector is preferable than the fixed throat ejector.

$T_g(^{\circ})$	A_r	E_m (%)	Q_g (kW)	Q_e (kW)	COP
90	7.2	57.0	9.82	4.27	0.43
100	9.4	60.02	9.62	4.36	0.45
110	12.0	68.3	9.42	4.67	0.50

Additionally, the main nozzle's movable spindle has a significant impact on the pressure there. When the generator temperature is high, a considerable amount of A_r reduces the pressure at the main nozzle's exit, which causes the primary flow to exhibit overexpansion

tendencies. On the other side, fixed throat ejectors tend to under-relax at high generator temperatures because a high pressure builds up at the primary nozzle's exit, which is bad for COP. Similar to this, when T_e is big and T_c is small, an over-expansion flow may be seen at a large A_r and a small A_r , respectively. Because of this, VTEJ performs quite well.

3.3 Optimal VTEJ performance and generator temperature

The COP performance fixed throat area ejectors at various generating temperatures is displayed in Fig. 2. There is a generating temperature that is ideal for any ejector at which the COP is highest. This conclusion concurs with that of [16]. Increases in primary flow rate cause an increase in heat supply to the generator and, as a result, a fall in the COP when the generator temperature rises the ideal value. The operating situation may switch from the choked to unchoked condition or even have a reversed flow, causing a quick decline in the COP, however, whenever the generating temperature is lower than the ideal value. The line that connects the highest COP with varied throat areas is shown in Fig. 2 as a black dotted curve. The link between COP and throat area as the generator temperature ranges for the VTEJ is seen by this optimal performance curve. To keep the VTEJ operating at its best performance when the generator temperature changes, the throat area should be changed in accordance with this relationship. Fig. 2 further demonstrates that increasing the throat area ratio will improve performance and increasing the ideal COP when the generator temperature rises. Comparisons of the cooling load and heat supply for fixed or variable throat ejectors are shown in Fig. 3 and 4. Figures 3 and 4's black dotted curves illustrate the ideal cooling load and heat supply for the VTEJ as a function of generator temperature.

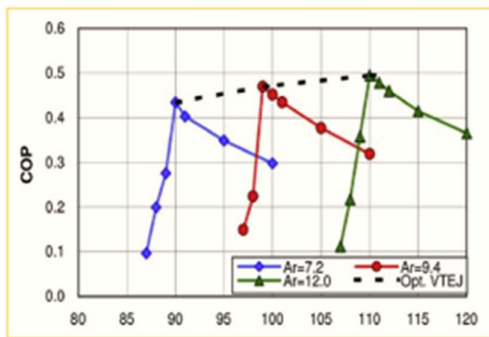


Fig. 2 Comparison of the COP for the $T_c=35$ °C and $T_e=15$ °C variable and fixed throat ejectors.

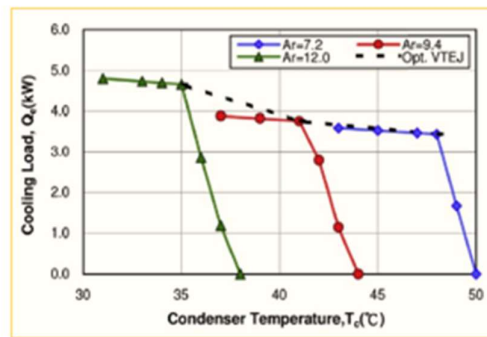


Fig. 6. cooling loads of various A_r values at $T_s=110$ °C and the value of the $T_a=15$ °C

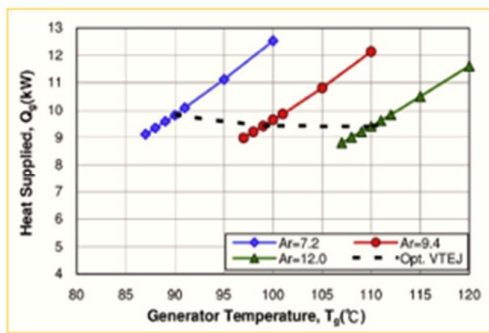


Fig. 4. Comparison of the Heat supply for the $T_c=35$ °C & $T_a=15$ °C variable and fixed throat ejectors

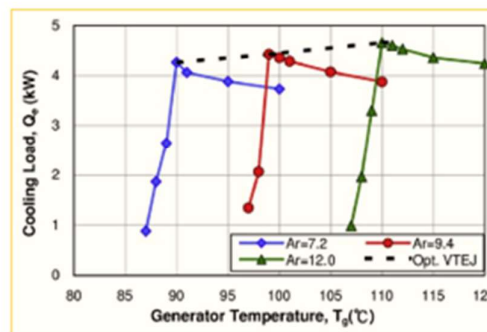


Fig. 3. Comparison of the Cooling load for the $T_c=35$ °C & $T_a=15$ °C variable and fixed throat ejectors

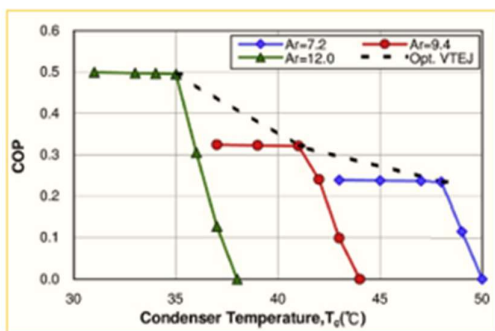


Fig 5. COP performance of the various A_r values at $T_g=110$ °C and the value of the $T_a=15$ °C

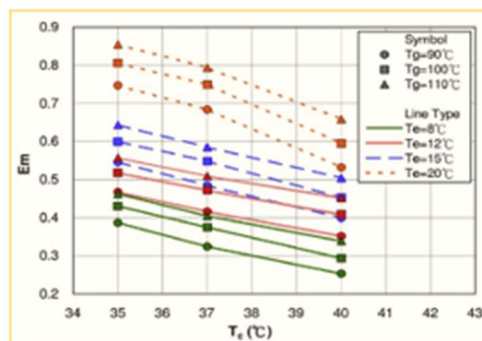


Fig 7. At various operating temperatures, the optimal entrainment ratio.

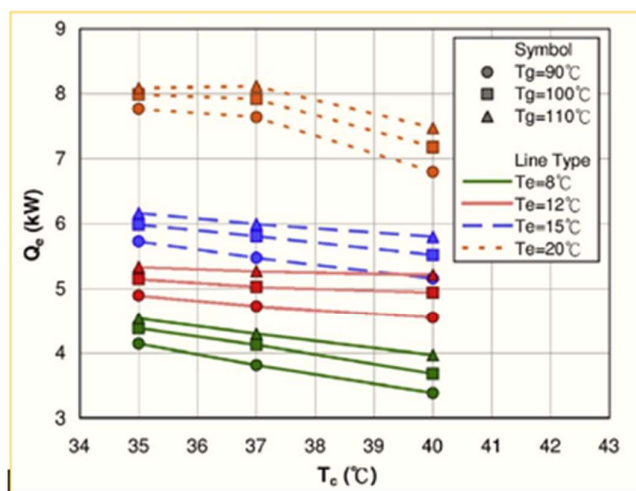


Fig 8. COP maxima at various operating temperatures.

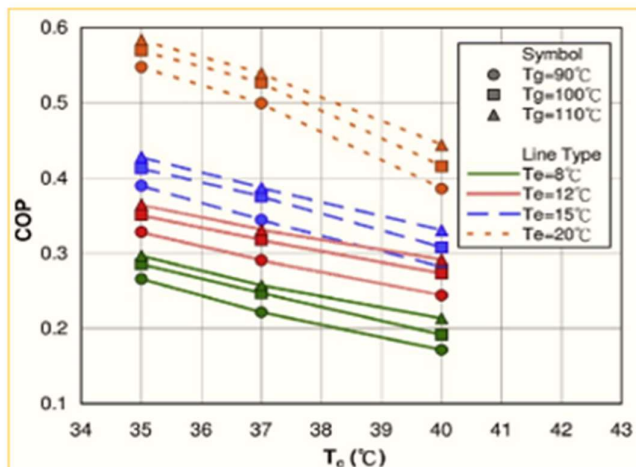


Fig 9. The best cooling load for various operating temperatures.

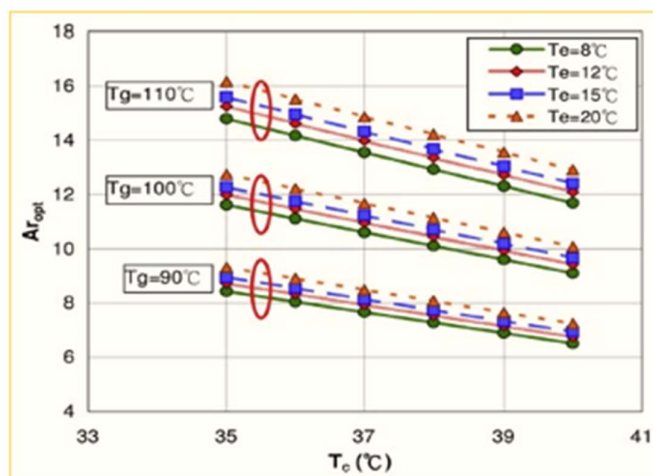


Fig 10. At various operating temperatures, the optimal throat area ratios (Ar_{opt}).

3.4 Condenser temperatures' impact on ideal VTEJ performance

Three fixed throat area ejectors are shown in Fig. 5 with the COP plotted against the condenser temperatures. Despite a modification in the condenser, the COP maintains its maximum value when the ejector is operating in the choked state, temperature.

All three ejectors work in the choked mode when the condenser temperature drops below 35 C, and a larger throat area ratio results in a higher COP. The Ar 14 12.0 ejector has the highest COP, as can be observed. The Ar 14 12.0 ejector runs in the unchoked condition when the condenser temperature is between 35 and 41 C, causing a quick decline in the COP, while the other two ejectors, which have smaller throat area ratios, continue to function in the choked state. Therefore, among these three ejectors, the one with Ar 14 9.4 has the greatest COP. The ejectors with Ar 14 9.4 and 12.0 work in the reversed position when the condenser temperature is between 41 and 48 C, which prevents the fluid in the evaporator chamber from being drawn into the mixing chamber and leads to ejector failure. As a result, the ejector with Ar 14 7.2 only functions when it is clogged. For varied throat area ratios, Fig. 6 displays the cooling load as a function of condenser temperatures.

The cooling demand barely little changes since the condenser temperature is below the critical temperature. In other words, while the ejector runs in the choked condition, the cooling load stays almost at its maximal value regardless of a change in the condenser temperature. In conclusion, if the ejector runs in the choked condition, altering the throat area may result in the maximum COP and cooling load when the condenser temperature fluctuates. In other words, the condenser temperature is below the critical point. The critical condenser temperature for an ejector with a certain throat area is therefore likely to be the same as the ideal condenser temperature, it seems reasonable to presume. All of the optimal positions are connected by the black dotted arc in Figures 5 and 6. These are the ideal COP curves for a VTEJ that is operating with a proper throat area ratio that has been modified to account for changes in condenser temperatures. It also demonstrates that, in order to attain the best COP, the throat area ratio should be raised when the condenser temperature drops, and vice versa.

3.5 Improvement of the VTEJs

The suggested solar-powered ejector refrigeration system is intended to function at T_g , T_e , and T_c of 90, 80, and 35, 400C, respectively. The best operational performance of the VTEJ under certain operating circumstances is discussed in this section. The ideal E_m , COP, and cooling load of the VTEJs are shown in Figs. 7-9, respectively. In these diagrams, the symbol denotes the temperature of the generator, while the line type denotes the temperature of the evaporator. The COP, E_m , and cooling load rise when the generator temperature is raised while the evaporator and condenser temperatures remain constant. The COP, E_m , and cooling load all rise when the evaporator temperature is raised while the temperatures in the generator and condenser remain constant.

As can be seen in Fig. 9, the Q_e often rises as the T_c falls. According to Section 3.4, when the condenser temperature T_c drops, the throat area ratio A_t should rise in order to attain the best COP. Because of the wide effective area and significant secondary flow caused by a small A_t . Notably, when T_c increases from 35 0C to 37 0C at $T_e=20$ 0C and $T_g=110$ 0C, Q_e marginally increases before dropping off with the increase in T_c , which is unusual from previous results. The throat area ratio A_t at $T_c=35$ 0C is lower than it is at $T_c=37$ 0C, as described in Sec. 3.4, indicating a lesser secondary flow. As a result, backflow occurs at T_c 14 35 0C as a result of a big T_e and a small A_{ton} the flow that can enhance the primary flow's overexpansion. Backflow reduces the Q_e at $T_c=35$ 0C in comparison to $T_c=37$ 0C. In addition to the ideal E_m , COP, and cooling load for ideal VTEJs, the ideal throat area ratio is also attainable. The formulae are introduced on an Excel worksheet in this article in order to acquire the linear regression parameters.

$$Ar_{opt} = 0.717T_g - 0.02T_e + 0.702T_c + 0.00204T_gT_e - 0.01185T_gT_c - 0.00257T_eT_c - 4395$$

The following regressive equation establishes a relationship between Ar and the operational temperatures. The equation's maximum inaccuracy is 3.0 percent. The optimal throat area ratio for various operation temperatures is depicted in Fig. 10. It demonstrates that when T_g and T_e are held constant, the throat area ratio drops linearly as the condenser temperature rises. As the generator temperature rises or falls, the throat area ratio correspondingly drops, as seen in the table below. Using the regressive equation, the throat area ratio may be changed if the temperature of the generator, evaporator, or condenser varies.

4. Conclusion

The suggested solar-driven ejector refrigeration system may operate at a different temperature depending on the amount of sun irradiation. When the temperature of the generator, evaporator, or condenser varies, the traditional fixed throat ejector may operate inefficiently or even break down. This paper suggests a variable throat ejector to enhance ejector performance and evaluates its performance using CFD simulations. The findings of this investigation are as follows. Although it may be overdesigned and costly, an ejector with a bigger throat area and solar collector offers a broader working range of generator temperatures. In contrast, reducing the throat area restricts the generator's temperature range, which may prevent the system from using solar energy as a heat source.

The variable throat ejector may be adjusted to the matching ideal throat area ratio if the operating temperature changes. This enables the system to operate at its best. In this work, a regressive equation is presented that connects the ideal throat area ratio to the operating circumstances at $T_g = 95-1150\text{C}$, $T_e = 9-220\text{C}$, and $T_c = 30-450\text{C}$. If the temperature of the generator, evaporator, or condenser is known from the standpoint of actual operation, the ejector may be modified using the regressive equation to the matching ideal throat area ratio.

References

1. K. Braimakis, "Solar ejector cooling systems: A review," *Renewable Energy*, vol. 164, pp. 566-602, 2021.
2. J. M. J. G. V. D. a. A. P.-M. Luján, "Optimization of the thermal storage system in a solar-driven refrigeration system equipped with an adjustable jet-ejector," *Journal of Energy Storage*, vol. 45, p. 103495, 2022.
3. V. S. V. J. S. V. D. a. A. C. O. Van Nguyen, "Applying a variable geometry ejector in a solar ejector refrigeration system," *International Journal of Refrigeration*, vol. 113, pp. 187-195, 2020.
4. J. V. D. L. M. G.-C. a. A. P.-M. Galindo, "Numerical evaluation of a solar-assisted jet-ejector refrigeration system: Screening of environmentally friendly refrigerants," *Energy Conversion and Management*, vol. 210, p. 112681, 2020.
5. D.-W. Sun, "Variable geometry ejectors and their applications in ejector refrigeration systems," *Energy*, vol. 10, pp. 919-929, 1996.
6. B.-J. C. B. J. a. F. L. H. Huang, "Ejector performance characteristics and design analysis of jet refrigeration system," *The American Society of Mechanical Engineers*, vol. 107, no. 3, pp. 792-802, 1985.
7. B.-J. a. J. M. C. Huang, "Empirical correlation for ejector design," *International Journal of Refrigeration*, vol. 22, no. 5, pp. 379-388, 1999.
8. Y. W. C. C. W. a. Y. L. Zhu, "Shock circle model for ejector performance evaluation," *Energy Conversion and Management*, vol. 48, no. 9, pp. 2533-2541, 2007.
9. K. W. S. M. B. T. S. a. S. A. Pianthong, "Investigation and improvement of ejector refrigeration system using computational fluid dynamics technique," *Energy Conversion and Management*, vol. 48, no. 9, pp. 2556-2564, 2007.
10. H. D. J. H. L. T. S. a. S. M. Kim, "Computational analysis of a variable ejector flow," *Journal of Thermal Science*, vol. 15, no. 2, pp. 140-144, 2006.
11. V. a. Y. A. Eveloy, "Thermodynamic Performance Investigation of a Small-Scale Solar Compression-Assisted Multi-Ejector Indoor Air Conditioning System for Hot Climate Conditions," *Energies*, vol. 14, no. 14, p. 4325, 2021.
12. X. W. Z. S. A. O. a. S. B. R. Ma, "Experimental investigation of a novel steam ejector refrigerator suitable for solar energy applications," *Applied Thermal Engineering*, vol. 30, no. 11-12, pp. 1320-1325, 2010.
13. K. S. S. a. Y. Y. Zhang, "Numerical investigation on performance of the adjustable ejector," *International Journal of Low-Carbon Technologies*, vol. 5, no. 2, pp. 51-56, 2010.

14. M. H. N. Z. A. a. M. B. Hamzaoui, "Experimental study of a low grade heat driven ejector cooling system using the working fluid R245fa," *International Journal of Refrigeration*, vol. 86, pp. 388-400, 2018.
15. B. J. S. L. C. V. O. P. a. K. O. S. Huang, "Theoretical and experimental investigation of the performance characteristics of an ejector cooling machine operating with refrigerant R245fa," In *The 23th IIR International Congress of Refrigeration*, 2011.
16. T. a. S. A. Thongtip, "An experimental analysis of the impact of primary nozzle geometries on the ejector performance used in R141b ejector refrigerator," *Applied Thermal Engineering*, vol. 110, pp. 89-101, 2017.
17. Talpada, JAGDISH S., and P. V. Ramana. "The theoretical analysis of H₂O-LiBr absorption refrigeration system using Al₂O₃ nanoparticles." *International Journal of Mechanical and Production Engineering Research and Development (IJMPERD)* Vol 9 (2019): 303-322.
18. Moorthy, CH VKNSN, et al. "Computational analysis of a CD nozzle with 'SED' for a rocket air ejector in space applications." *International Journal of Mechanical and Production Engineering Research and Development (IJMPERD)* 7.1 (2017): 53-60.
19. RAO, P. SRINIVASA, CH VKNSN MOORTHY, and V. SRINIVAS. "Numerical investigations for the effect of cold and hot air on various parameters of flow through a super sonic nozzle at higher altitudes." *International Journal of Mechanical and Production Engineering Research and Development* 7.6 (2017): 21-44.
20. Saleh, B., and MS YOUSSEF. "Parametric analysis of an ejector refrigeration cycle activated by renewable energy." *International Journal of Mechanical and Production Engineering Research and Development (IJMPERD)* 9 (2019): 1143-1156.
21. Govardhan, D., and B. Praveen. "Design And Analysis Of Two Throat Wind Tunnel." *International Journal of Mechanical and Production Engineering Research and Development (IJMPERD)* 8. 1, Feb 2018, 513 520.
22. Khan, Sher Afghan, Abdul Aabid, and Maughal Ahmed Ali Baig. "CFD analysis of CD nozzle and effect of nozzle pressure ratio on pressure and velocity for suddenly expanded flows." *International Journal of Mechanical and Production Engineering Research and Development* 8.3 (2018): 1147-1158.